ARCHIVE PAPER
Published in Winter 1983/84
Vol. 17, No. 4

A Range-Gated Laser System for Ocean Floor Imaging

Timothy H. Dixon
Jet Propulsion Laboratory
Pasadena, California

Thomas J. Pivirotto
and
Robert F. Chapman
Jet Propulsion Laboratory
Pasadena, California

Robert C. Tyce
Marine Physical Laboratory
Scripps Institution of Oceanography
La Jolla, California
and
Graduate School of Oceanography
University of Rhode Island
Naragansett, Rhode Island

We describe tank studies which show that a copper chloride laser is a good illumination source for a deep ocean imaging system. The laser is naturally pulsed (~20 ns pulse width) at repetition rates of 10 to 20 kHz, and operates with high (1%) efficiency in the blue-green window for optimum transmission in water. A range-gated, scanning imaging system based on this laser can operate with input power of a few hundred watts, obtaining 100m wide digital image coverage of the sea floor from altitudes of 50 m. Measurements of range (bathymetry) and particulate matter distribution within the water column are also possible.

INTRODUCTION

A seafloor search or survey operation in the deep ocean often consists of mapping with side-looking sonar followed by highly selective photography.[1] Typically a 100 kHz sonar is towed 50 meters above the seafloor by a surface ship travelling at 2 knots (1 m sec^{-1}), creating kilometer-wide acoustic images at high search rates (~4 km^2 hr^{-1}). However, sonar reflection tends to be specular and most operational systems also have limited angular (azimuth) resolution. Photographs are therefore taken of specific areas of interest to provide additional information. Photography provides accurate identification of sonar targets since most objects are diffuse scatterers of light. Optical surveying must be done from altitudes of $\leq$ 20 m utilizing high-power strobe lights for illumination.[2] The short-range nature of ocean photography results from the severe attenuation of light in water. Simultaneous long-range sonar work is precluded due to the reduced altitude.

Light attenuation in seawater is caused by both molecular absorption, which dominates at longer wavelengths, and small particle scattering dominant at shorter wavelengths. These effects cause strong attenuation at most electromagnetic wavelengths, with a minimum in the blue-green optical band (Figure 1). In addition, backscattered light from large particles in the near field reduces signal-to-noise ratio (contrast) at the receiver. This is minimized by separating the light source and receiver and causing their common field of view to overlap only near the target.

There are also operational problems associated with acquisition of optical ocean floor imagery. Television systems are hampered by the low bandwidth of long co-axial cables, requiring low scan rates and/or low resolution. Film cameras are limited in areal coverage by film magazine size. Typical light sources are strobes or incandescent lamps, which have limited power output and are inefficient, spreading energy over a broad range of wavelengths and angles.

A scanning laser has several advantages over conventional light sources for illumination in the oceanic environment.[3] First, lasers are inherently narrow band systems and can concentrate energy in the minimum loss blue-green spectral region. Second, lasers are collimated, so that energy is concentrated in angle. Losses associated with spherical spreading (proportional to $1/r^2$) apply in one direction only, after scattering by the target. Beam scanning can be employed for the required areal coverage. Third, some lasers operate as naturally pulsed light sources with very short pulse length. Backscattered light from particulate matter in the water tends to limit effective range independent of lighting power. Range-gated receivers can utilize a pulsed signal to minimize and/or measure backscattered light. Altitude (range) can also be determined in a quantitative manner, generating an unambiguous three-dimensional description of the target swath.

The copper halide laser developed at the Jet Propulsion Laboratory (JPL) is an efficient, naturally pulsed laser. This paper describes feasibility tests for oceanographic applications, in particular for a range-gated scanning laser imaging system. The study included measurements of laser efficiency, and beam divergence and attenuation for different water clarities. The amount of light backscattered from several rock types at various incidence angles was also determined.

THE COPPER CHLORIDE LASER

Copper vapor lasers were originally developed for high power and efficiency in the visible spectrum.[4,5] To improve reliability and lifetime, JPL developed a series of lasers with copper halide lasants. These com-

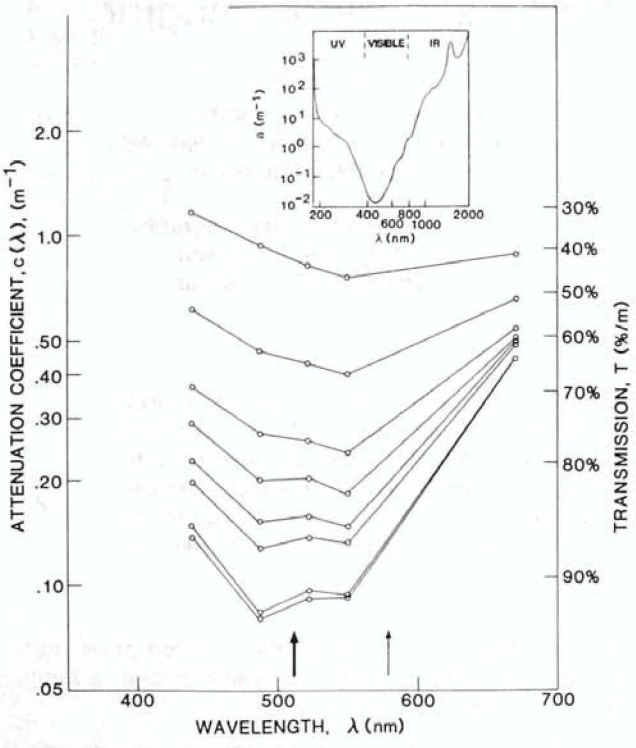

Figure 1. Total beam attenuation coefficient (c) as a function of wavelength (λ) for a representative variety of water clarities measured during this study. c(λ) is a measure of both particle scattering and molecular absorption of light and was varied by addition of an aluminum hydroxide-magnesium hydroxide mixture. The transmission per meter (T) is related by: $T = I/Io = e^{-c(\lambda)L}$ for L = 1m. Note shift of minimum toward yellow for lower clarity water.[14] The thick and thin arrows represent wavelengths of the laser's green and yellow emissions respectively. Insert shows the molecular absorption coefficient (a) for electromagnetic radiation in seawater (modified from McAlister and McLeish 1965).

pounds supply vapor-phase Cu at reduced temperature.[6] In a low pulse repetition rate (PRR) double pulsed system, the first pulse causes halide dissociation, while the second produces population inversion and lasing. Pulse energies of ~ 10mJ are obtained in this mode.[7] Higher efficiencies are obtained with continuously pulsed systems operating at high PRR (≧ 10^4Hz).[8,9,10]

The laser system used here is a continuously pulsed, copper chloride (CuCl) laser. It consists of an insulated quartz tube 1 m long and 2.5 cm diameter in a metal housing. The tube is fitted with Brewster windows at each end, two electrodes for excitation, two ports for neon buffer gas introduction and removal, and a small CuCl reservoir with integral heater. Associated equipment consists of a high voltage power supply and discharge circuits, CuCl heater electronics, neon buffer gas and flow control hardware, and pump hardware for maintenance of tube vacuum.

The characteristics of this laser most useful for oceanographic applications are summarized below.

Wavelength

Laser output is at 510.6 nm (green) and 578.2 nm (yellow). The green/yellow ratio (≃ 1.2 — 1.8 in our experiments) can be increased by adjusting the CuCl reservoir temperature, PRR, and discharge circuit voltage.[11] The green wavelength is in the band of minimum attenuation in clear sea water (Figure 1).

Power Efficiency

The CuCl laser has an overall power efficiency of nearly 1%. This is low relative to other light sources, but these have wide bandwidths and lose power outside the blue-green window to attenuation. No power losses are incurred in this laser by wavelength shifters, since the natural emission is blue-green.

Power Output

Average power output at a PRR = 10 kHz was varied between 4 and 8 W during our tests (pulse energy 0.4 — 0.8 mJ). The maximum power output achievable with this laser is 17 W (pulse energy = 1.7 mJ).

Pulse Duration

For both green and yellow spectral lines, pulse duration between half power points is about 20 ns. Simple shape analysis of the return signal (e.g. leading edge detection) should allow 1 m range resolution. For greater range resolution, pulse duration can be reduced to 5 ns with alternate pulse discharge circuitry and the use of helium buffer gas.

Gain

The CuCl laser is a high gain system due to the high excitation cross section and short spontaneous life time of the 2_P state of copper. As a result, the system is not sensitive to alignment of the end mirrors, a very desirable "field" characteristic. The system will even lase without mirrors.

Pulse Repetition Rate (PRR)

The CuCl laser operates efficiently with a PRR between 10 and 20 kHz, allowing rapid scanning of relatively wide swaths of ocean floor.

Beam Diameter and Divergence

For the laser tube used here (2.5 cm diameter), beam diameter at the output coupler, defined by the half power points, was about 25% of the tube inside diameter. Under these conditions the iris diameter through which 90% of beam power passes is about 45% of the tube inside diameter.

With a stable resonator consisting of a concave, fully reflecting mirror with a radius of curvature (4 to 6 m) greater than the cavity length, and an uncoated optical flat for an output coupler, beam divergence half angle is about 2 mrad. With an unstable, confocal resonator consisting of the same 100% reflector at the rear and

a small (1-2 mm diameter) convex mirror in front, beam divergence is about 0.1 mrad.

With a beam divergence of 2 mrad, beam diameter at 50 m is less than 25 cm. This could provide a high resolution scanning imaging system with 500 or more picture elements (pixels) spanning 100 m of the sea floor (i.e. pixel size ~ 20 cm).

Endurance

The CuCl laser is a highly reliable system. Eight hours of continuous operation were routine for our experiments. Endurance tests [11] suggest that at least 100 hours of continuous operation can be expected.

EXPERIMENTAL RESULTS

Experimental Set-up

The 13m-long test tank at the Visibility Laboratory of Scripps Institution of Oceanography was used for this experiment (Figure 2). The laser beam was vectored into the tank through a large lucite window with two high quality mirrors. After traveling through the tank and striking a target, backscattered light traversed the tank again for collection at the source window.

Backscattered light reaching the lucite window was collected with a 25 cm diameter Fresnel lens. A collimating lens and a series of calibrated filters directed the light into a photomultiplier tube (PMT) connected to a fast oscilloscope. For all target configurations, the normal to the target surface, the incident ray and the collected ray formed a horizontal plane.

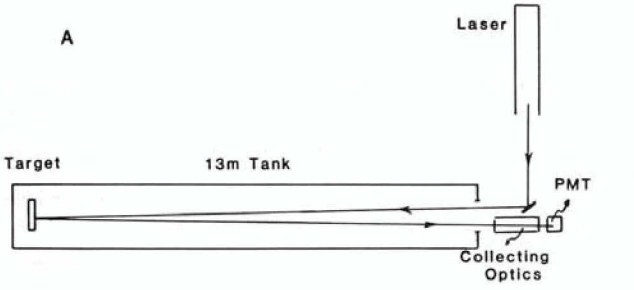

Figure 2a. Sketch of the experiment set-up.

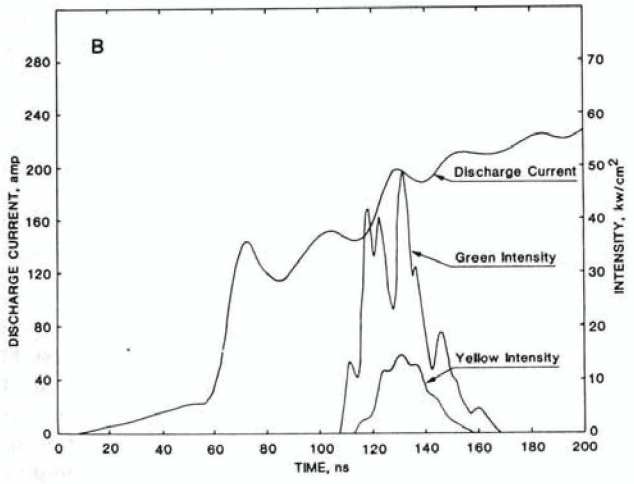

Figure 2b. Temporal pulse structure for both green and yellow laser output compared to discharge current pulse.

Collecting optics had two configurations. For measurement of target properties, input beam and collecting optics had maximum separation (~15 cm) to minimize near-field backscatter. By measuring target properties at different distances, the distance where the two fields of view began to overlap was found to be about 7m. For determining near-field backscattered intensity as a function of water clarity, a coaxial system was employed, with the laser beam directed down the tank by means of a mirror positioned at the center of the collecting lens.

The PMT used for these tests was an RCA #1P28. Manufacturer's specifications for the quantum efficiency of the 1P28 are 5.5% at a wavelength of 510.6 nm and 1.9% at 578.2 nm. Current amplification is 2.5×10^6 at 1000 V. A low inductance voltage divider (50 ohm anode load) preserved the fast (2ns) rise time of the 1P28, and minimized signal fall time. Temporal structure of the laser pulse could be followed with very little distortion.

Water clarity could be increased by continuously circulating the water through a commercial swimming pool filter, and was monitored with a transmissometer.[12] Transmission in the blue-green band reached a maximum of 92% m^{-1}, slightly less than the clearest ocean water.[13] To study backscatter and beam losses at reduced clarity, the filter was bypassed and 1-2 gm of a commercial mixture of $Mg(OH)_2$ and $Al(OH)_3$ were added in increments.

Beam Divergence Tests

Beam divergence does not change significantly with water clarity (Figure 3). The full angle beam divergence in air is about 4 mrad, yielding a beam diameter of 10 cm at a distance equivalent to the tank exit window (~18 m from the laser). This is almost identical to the diameter measured in water (Figure 3).

Effect of Water Clarity on Reflected Power

Measured peak power as a function of water clarity for both green and yellow wavelengths is shown in Figure 4. These results were obtained with co-axial optics and a white diffuse reflector at the far end of the tank. Reflected peak pulse power was recorded at each level of transmission through green and yellow narrow band filters. Data were adjusted for filter losses. Theoretical signal strength (Figure 4) is calculated by adjusting for losses at target and receiver, and for attenuation in water:

$$W_r = \frac{W_t\, e^{-2c(\lambda)L}\, R \cos \Phi\, (D^2/4)\tau}{L^2}$$

where

W_r = received peak pulse power

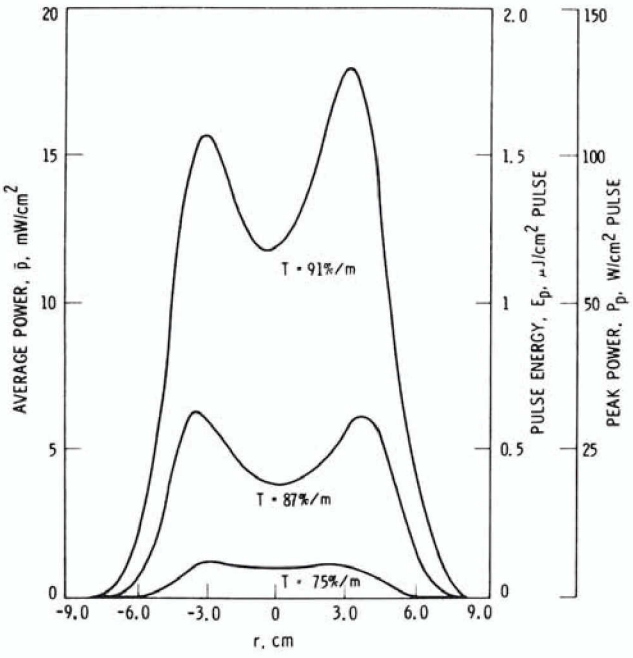

Figure 3. Beam width as a function of water clarity. Profiles represent strip chart recordings of radiometer sweeps outside the window at the target end of the tank. Dip in beam center is a property of the laser.[11] Radiometer measured average beam power per unit area ($\bar{P}$). Pulse energy per unit area (E_p) is given by: $E_p = \bar{P}/PRR$ where PRR = 10 kHz. Peak pulse power (P_p) is given by $P_p = E_p/T$ where T = pulse duration = 20 ns.

W_t = transmitted peak pulse power = 4.8×10^4 watts
L = tank length = 13m
R = target reflectivity = 88%
Φ = the angle between the normal to the target surface and the laser beam = 0°.
D = receiver aperture diameter = 0.25 m
τ = receiver efficiency = 35%

c(λ) is the total beam attenuation coefficient, and is a measure of combined losses due to scattering and absorption. It is also related to the net transmission per meter (see Figure 1). For water clarities above ~70% transmission per meter, there is excellent agreement between theoretical and measured received power.

Rock Reflectance Measurements

Quantitative values of rock reflectance as a function of incidence angle are required for performance estimates for a scanning laser imaging system. A large body of literature exists on the reflectance characteristics of natural and manmade materials.[14] The quantity measured is generally the bi-directional reflectance at a particular wavelength. This measurement utilizes a collimated incident beam normal to the surface or at specified angles, and a detector with limited field of

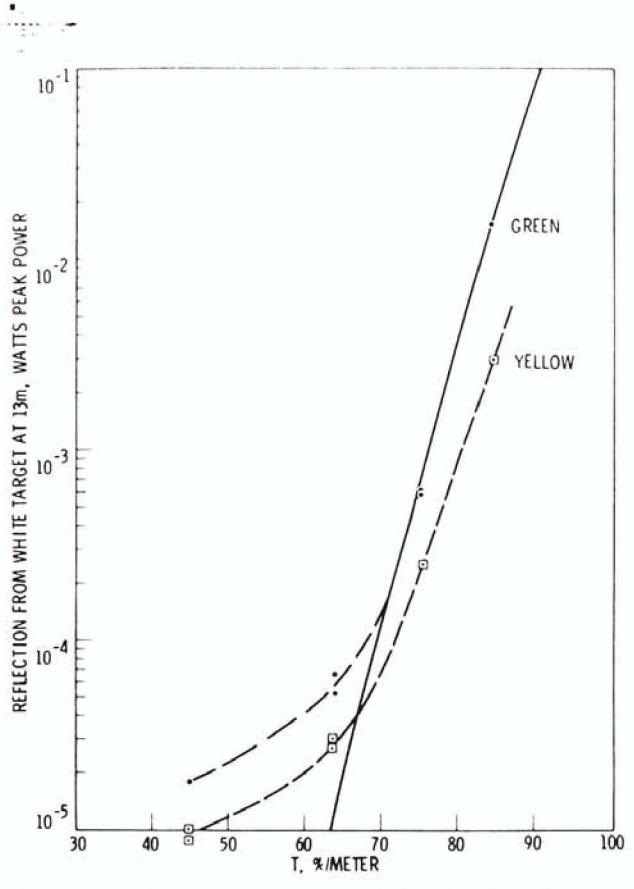

Figure 4. Peak pulse power received as a function of water clarity (transmission, T) for green and yellow laser emissions. Dashed lines connect data. Solid line is the theoretical received power calculated according to equation 1 in the text. Values for T are estimated from data in Figure 1 at λ = 510.6 nm.

view at some fixed angle off normal, typically 30° or 45°. To the extent that the test materials reflect the incident beam equally in all directions, such measurements can be valuable guides to reflectance under any illumination geometry. However, natural rock surfaces may exhibit specular reflection characteristics. In self-illuminating imaging systems, the outgoing beam and reflected light received are nearly coincident, and "0-45°" bi-directional reflectance measurements may not adequately characterize the surface. In addition, reflectance values are highly dependent on incident wavelength, and few measurements have been made at the CuCl laser's frequencies.

We therefore measured the reflectance of rock samples under conditions approximating imaging system geometry. Six rock samples, crudely representative of expected marine lithologic variation, were tested for reflectance at various indicidence angles. Most samples were large slabs ≥50 cm in diameter. Samples were mounted on a rotating holder which could be set to pre-determined incidence angles from 0° to 56°. Samples included: (a) a sedimentary rock (cream to

reddish colored sandstone; (b) low grade metamorphic rocks (green slate, black slate and a dark mica-schist); and (c) igneous rocks (gabbro and a red basaltic scoria) (Table 1). Submerged reflectance values are also listed in Table 1. Reproducibility of measurements on individual rocks was better than ± 1.0% reflectance for a given sample orientation. Standards were calibrated with a "0-45°" measurement geometry, while a "0-0°" geometry was used for the samples. This should not bias our sample reflectance measurements as long as the standard targets are diffuse reflectors. Figure 5 suggests that this is so: the standard targets show much less variation in reflection with incidence angle or target orientation than do natural rock surfaces.

The relative variation in reflectance among the samples at normal incidence is similar for air and water. Light-colored or green samples are most reflective, and dark-colored or red samples are least reflective under green light. The basalt scoria has the lowest absolute reflectance at normal incidence (3.8% — 4.0). Its low reflectance under green illumination is consistent with its red color and highly vesicular nature. The vesicles are approximately spherical, and would trap and absorb most incident light at any angle. Green slate had the highest reflectance (8.0-8.6%).

Two types of reflectance variation with incidence angle were observed. The gabbro and sandstone samples closely follow Lambert's law for diffuse reflectors. The amount of light reflected back to the PMT therefore depends only on the area illuminated as seen by the detector, here a constant. In contrast, the slate and mica-schist reflectances exhibit some angular dependence. The amount of light received by the PMT at incidence angles off perpendicular is significantly less for these samples than for a diffuse reflector, i.e. the surfaces exhibit some specular reflectance (Figure 5). These samples all contain minerals with tabular or platy crystal structures, such as clays and micas, which can act as specular reflectors. Moreover, these minerals will generally be aligned parallel to the macroscopic cleavage surface. The green slate exhibited the most sensitivity to incidence angle, with backscatter intensity decreasing by a factor of two between normal incidence and 45°.

Near-Field Backscatter Measurements

Near-field backscattering of light is of interest because: (a) it limits signal-to-noise ratio (contrast); and (b) it provides information on volume distribution of particulate matter in the water column. Measurements were made of backscattered light intensity for different values of water clarity using co-axial collecting optics. All light collected from 4 meters to the end of the tank entered the PMT. For shorter ranges the divergence of most of the collected light was too great to be focused into the PMT. Reference targets were diffuse reflecting plates painted either white (for lower clarity water) or black (for higher clarity water).

TABLE 1

Rock Type	Mineralogy[1]	Surface[2]	Comments	% Reflectance[3]
Green Slate Black Slate	Quartz, chlorite, sericite, minor feldspar	Foliated cleavage plane	Green = high chlorite, no carbonate Black = low chlorite, minor carbonate	8.0-8.6 6.4-7.3
Gabbro	Plagioclase, green amphibole, minor chlorite, relict clinopyroxene, assessory magnetite	Smooth, cut	———	6.7-6.9
Sandstone	Quartz	Smooth bedding plane	Carbonate, hematite cement, some pressure solution	5.4-6.3
Schist	Quartz, muscovite, chlorite, epidote	Clevage plane, minor foliation	———	5.4-6.0
Red Basalt Scoria	Plagioclase microlites, rare large olivine phenocrysts, dark fine grained groundmass	Very rough	30% vesicles, .3-3 mm diameter	3.8-4.0

[1] Determined by thin section analysis, or for fine grained slates, by x-ray diffraction.

[2] All surfaces are natural cleavage or bedding planes except gabbro, with artificial cut surface.

[3] Calculated by comparison to four standard gray or black matte surfaces with 0.75%-15.8% reflectance, as measured by a Gardner "Colorguard" 0-45° reflectometer.

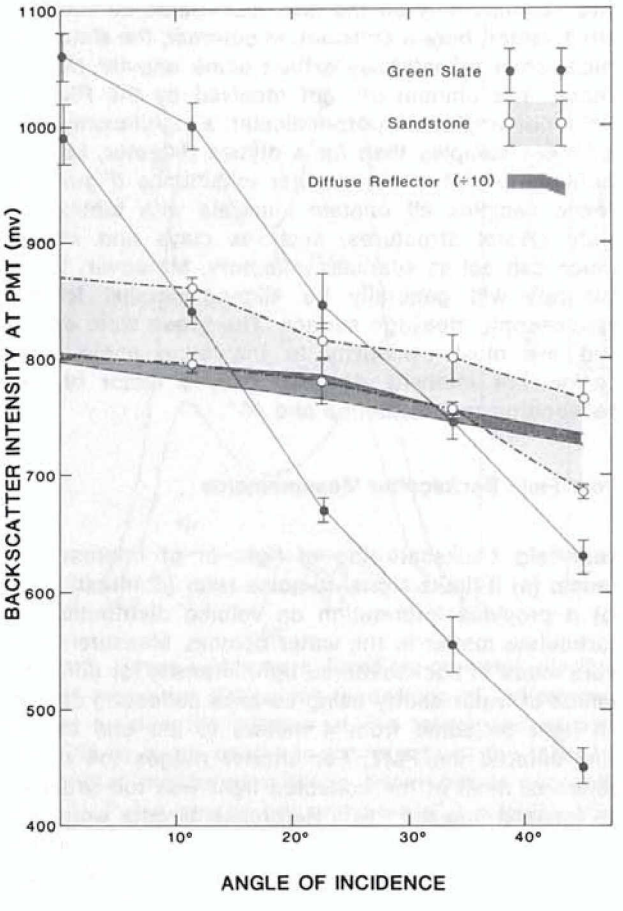

Figure 5. Variation in light intensity backscattered to the photomultiplier tube (PMT) as a function of target orientation. Two rock samples, with reflectance values at normal incidence of 8.0%-8.6% (green slate) and 5.4%-6.3% (sandstone) are compared to a white matte target (3M "White Velvet" diffuse reflecting paint, ~ 85% reflectance). White target data were collected with an additional neutral density filter (10% transmission) in front of the PMT. Higher and lower values for individual samples at a given incidence angle represent two orthogonal sample orientations, obtained by rotating the sample about the normal to the surface. These differences likely represent the influence of surface texture on backscatter. Error bars on individual rock measurements represent observed variation in backscatter with right versus left-handed rotation of the samples. The indicated field for the white reflector represents total observed variation with right vs left rotation and two orthogonal orientations.

The two rock samples indicated represent extremes in angular dependance observed in the six rock samples. The sandstone acts as a diffuse reflector, similar to the white matte target. Backscatter from these surfaces is not a strong function of incidence angle. In contrast, backscatter from the slate sample shows a strong angular dependance, decreasing by a factor of two from normal incidence to 45°.

Line tracings of oscilloscope displays during the backscatter experiment are shown in Figure 6 for various water clarities. Peaks near 120 ns represent backscatter from the target at 13 m, while the signal between 40 ns and 110 ns represents backscatter from particulates in the water between 4 and 13 m.

The major difference in received signal for various water clarities is the target strength. The backscatter from particulates shows a more subtle dependence on water clarity. In the near field (between 40 and 60 ns) a higher particulate content causes stronger backscattering of light. However, since the intensity at successively farther distances is strongly attenuated as water clarity is reduced, the backscattered signal from farther distances (60-110 ns) is also reduced. The best measure of particulates may not be an absolute signal strength from backscatter at some distance, but rather the relative slope of the return signal over a time range. This slope will be lower in clear water than in turbid water. Relative signal strength at two separate times can be precisely measured, so that a laser system designed primarily for ocean floor imaging could also function as a nephelometer.

DISCUSSION

The feasibility of a laser imaging system can be tested by estimating the strength of a light pulse at the receiver after interaction with the rock surface and attenuation by water. Our reflectance data suggest that most sea floor surfaces will reflect more than 5% of incident light over the range of incidence angles likely to be used in a scanning imaging system. Expected signal strength (S) at the receiver for normal incidence is:

$$S = \frac{N\, e^{-2cL} R A \tau}{\pi L^2}$$

where
- N = number of output photons per pulse = 2.6×10^{15} for 1 mj pulse of green light
- c = attenuation coefficient = .0834 m^{-1} (for T = 92%/m)
- L = height from bottom = 50 m
- R = rock reflectivity = 5%
- A = receiver area = .20 m^2 (50 cm diameter lucite lens or mirror)
- τ = receiver efficiency = 30%

This gives S ~2×10^5 photons. Many PMT's can detect signals as low as 10^2 photons, so the absolute signal level is adequate for our hypothetical imaging system.

PMT output can be characterized by Poisson statistics; variance in the number of photons arriving at the detector = $\sqrt{M}$ where M is the measured number,

i.e. roughly $2 \times 10^5 \pm 5 \times 10^2$ in this example. The relative uncertainty in the return signal is then $\pm \frac{\sqrt{S}}{S} \times 100 = \pm 0.2\%$. Hence the backscattered signal would have to change by more than ± 0.2% in order to be interpreted as a change in sea floor reflectivity. The signal-to-noise ratio (SNR) of the PMT is also governed by Poisson statistics and is given by the square root of the product of quantum efficiency and the number of photons received. Since both SNR and the minimum detectable change of sea floor reflectivity depend on the number of photons in the received pulse, S must be reasonably large ($> 10^3$ photons).

Total power consumption is largely determined by the laser's PRR. If we envision a 1 mJ laser system towed 50 m above the sea floor at a speed of 1 m sec^{-1} to produce sea floor images 100 m wide with 500 pixel resolution, then a PRR of 2.5 kHz is required. This implies an input power of 250 W, assuming efficiency comparable to our test laser. Such scaling studies are now being undertaken.

Figure 7 suggests the limitations of a scanning laser imaging system in terms of minimum water clarity and maximum range. If the imaging system were required to operate a minimum of 30 m above the bottom for operational safety and adequate field of view, then water clarity would have to be better than 83% m^{-1} to ensure some minimal level of return signal strength (~ 10^3 photons per pulse). Since most water masses

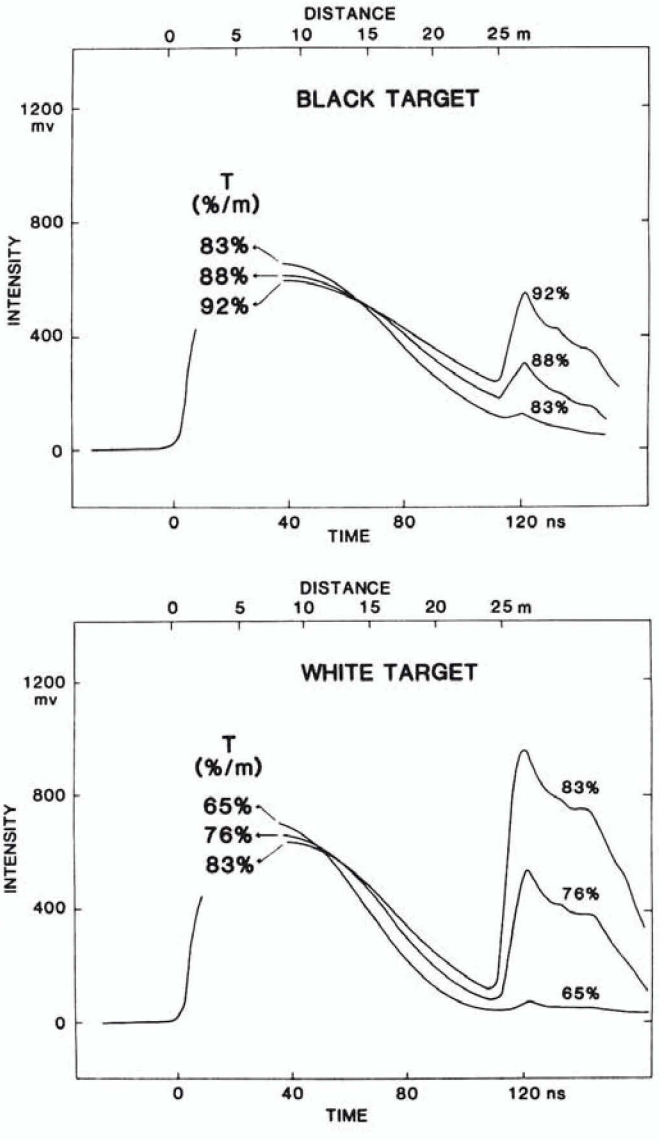

Figure 6a,b. Backscattered light intensity as a function of two-way travel time or distance (laser input-target-receiver) for several values of water clarity. T(%/m) is the measured transmissivity of the water. Figures represent line tracings of actual oscilloscope displays. A black target was used for higher values of water clarity (Figure 6a) while a white target was used at lower clarity (Figure 6b), to keep the strength of the return signal within the linear range of the PMT.

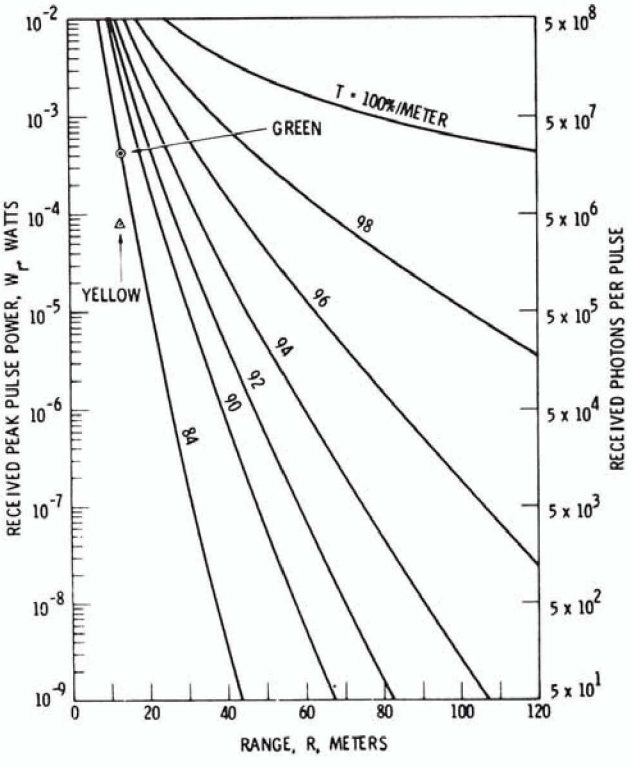

Figure 7. Received peak pulse power (W_r) for a scanning laser imaging system as a function of range (height from bottom) and water clarity. Values are derived from equation 1, assuming $W_t = 4.8 \times 10^4$W, $\tau = 35\%$ R = 2.38%, Φ = O, D = .25 m. Experimental result for a black diffuse target (R = 2.38%) at T = 84%/m and $W_t = 4.8 \times 10^4$ W is also shown. Photons per pulse (right side ordinate) calculated by multiplying W_r by pulse length (20ns) and dividing by energy of a green photon (3.89×10^{-19}j).

in the open ocean are clearer than this,[13] the CuCl laser appears to be an adequate illumination source for our hypothetical imaging system. A prototype unit is planned for use with a deeply towed sonar system. Tests are scheduled to begin in 1986.

ACKNOWLEDGMENTS

Roswell Austin, Director of SIO's Visibility Laboratory, gave timely suggestions and encouragement. Sherman Bloomer provided the gabbro sample. Albert Chapin was very helpful through many phases of the experiment, for which we are especially grateful. We thank William Grant for suggesting the use of equation 3, and Eric Shulenberger and an anonymous reviewer for helpful comments. Funding for this research was provided by JPL through the Director's Discretionary Fund.

REFERENCES

1. Tyce, R.C. and D.E. Boegeman. 1977. Integrating optics and sonar for a deeply towed vehicle. IEEE Marine Tech. Soc. 34A:1-6.
2. Buchanan, C.L. 1975. Sea-floor photography: Equipment and techniques. Oceanus 18:11-16.
3. Heckman, P.J., Jr., and P.D. McCardell. 1978. A real-time optical mapping system. Proc. Soc. Photo. Inst. Eng. 160:189-196.
4. Asmus, J.F. and N.K. Moncur. 1968. Pulse broadening in an MHD copper vapor laser. Applied Phys. Lett. 13:384.
5. Russell, G.R., N.M. Nerheim and T.J. Pivirotto. 1972. Supersonic electrical-discharge copper vapor laser. Applied Phys. Lett. 21:565.
6. Chen, C.J., N.M. Nerheim and G.R. Russell. 1973. Double-discharge copper vapor laser with copper chloride as a lasant. Applied Phys. Lett. 23:514-515.
7. Nerheim, N.M., A.A. Vetter and G.R. Russell. 1978a. Scaling a double-pulsed laser to 10 mJ. J. Applied Phys. 49:12-15.
8. Liberman, I., R.V. Babcock, C.S. Liu, T.V. George and L.A. Weaver. 1974. High-repetition-rate copper iodide laser. Applied Phys. Lett. 25:334-335.
9. Chen, C.J. and G.R. Russell. 1975. High efficiency multiply pulsed copper vapor laser utilizing copper chloride as a lasant. Applied Phys. Lett. 26:504-505.
10. Anderson, R.S., B.G. Bricks and T.W. Karras. 1977. Steady multiply pulsed discharge-heated copper-vapor laser with copper halide lasant. IEEE J. Quant. Electron. 13:115-117.
11. Nerheim, N.M., A.M. Bhanji and G.R. Russell. 1978. A continuously pulsed copper halide laser with a cable-capacitor Blumlein discharge circuit. IEEE J. Quant. Electron. 14:686-693.
12. Austin, R.W. and T.J. Petzold. 1975. An instrument for the measurement of spectral attenuation coefficient and narrow angle volume scattering function of ocean waters. Scripps Institution of Oceanography Ref. No. 75-25 (12 pp).
13. Duntley, S.Q. 1963. Light in the sea. J. Optical Soc. Am. 53:214-233.
14. Watson, R.D., W.R. Hemphill, T.D. Hessin, and R.C. Bigelow. 1974. Prediction of the Fraunhofer line detectivity of luminescent materials. Proc. 9th Symp., Remote Sensing and the Environment, Environmental Research Inst. Michigan 1959-1980.
15. McAlister, E.D. and W.L. McLeish. 1965. Oceanographic measurements with airborne infrared equipment and their limitation. *In* G.C. Ewing (ed.) Oceanography from Space, Woods Hole Oceanographic Institution, Ref. 65-10:189-214.